Worm structure in the modified Swift-Hohenberg equation for electroconvection

Yuhai Tu

IBM Research Division, T. J. Watson Research Center, P.O. Box 218, Yorktown Heights, New York 10598

An anisotropic complex Swift-Hohenberg equation is proposed to study pattern formation in electroconvection. In the subcritical regime, a localized state is found in two dimensions, which resembles the ''worm'' state observed in recent experiment by M. Dennin *et al.* [Phys. Rev. Lett. **77**, 2475 (1996); Science **272**, 388 (1996)]. In the corresponding one-dimensional model, a stationary pulse state is discovered, due to a nonadiabatic effect, and it is shown to explain the localization of the ''worm'' state in the two-dimensional model. Based on these results, we believe that the initial bifurcation should be subcritical where the ''worm'' state is observed, and further experiment is suggested to test this scenario. [S1063-651X(97)50110-3]

PACS number(s): 47.54.+r, 02.60.Cb, 47.20.Ky

The study of localized structures in nonequilibrium system has received a great deal of attention since being observed experimentally in binary-mixture Raleigh-Bénard convection (RBC) [1]. Even though binary-mixture RBC is a highly dissipative system, the localized structures behave much like solitons in integrable systems. On the theory side, Thual and Fauve [2] were the first to study the behavior of a subcritical complex Ginzburg-Landau equation and found that in certain parameter ranges, there are indeed localized pulse solutions. The basic ingredients for the existence of localized structure are (i) there has to be linear bistability, which guarantees the local stability of the peak and the tail of the pulse; (ii) nonlinear dispersion (the complex part of the coefficients for the nonlinear terms) is needed to stabilize the front connecting the peak and the tail of the localized solution. Much work has since been devoted along these lines to understanding the details of the experimental results [3,4].

Most of the experimental results in binary-mixture RBC were obtained in quasi-one-dimension, i.e., in a thin annulus [5]. Further efforts to extend these findings to a two dimensional (2D) system have not revealed any similar 2D localized state as in one dimension (1D), except for some time-dependent patchy structure [6] and some long time transients [7]. Recently, Dennin *et al.* [8,9] studied electroconvection in a nematic liquid crystal carefully. Depending on the electrical conductivity, they found that the pattern above onset is either a spatially extended spatial-temporal chaos (STC) state or some isolated localized state, which they named the ''worm'' state. The worm state is localized in the direction perpendicular to the director of the liquid crystal, but is extended in the parallel direction. The worm can move in the parallel direction. The internal structure of the worm seems to consist of both orientations of the linearly unstable oblique rolls, and the internal roll structure is moving relative to the motion of its envelope.

In this paper, we present a theoretical study of the intriguing localized worm pattern. Recently, there has been progress in constructing a microscopic model whose linear properties agree with those of the experiments [9]. However, to understand the electroconvection quantitatively from the full nonlinear microscopic equations is still a daunting task. Meanwhile, many of the fundamental qualitative questions remain unanswered, such as the reason for the existence of the worm state in the first place. For this purpose, we propose a phenomenological model to explain the formation of the worm state. As we show below, we have indeed found in our model a nontrivial localized state, whose structure and dynamics resemble those of the worm state in the experiment. We also demonstrate that the localization of the worm state is due to small scale physics (nonadiabatic effect), and, in fact, the corresponding 1D structure is a different kind of localized state. Experimental measurements are also suggested to test our theory.

The amplitude equation formalism that was used in [3] and related works [3,4] to study the pulse pattern in binary-mixture RBC in principle describes the large scale and long time behavior of the envelope of the pattern. For the problem at hand, the spatial extension of the worm state in the perpendicular direction is comparable to the basic wavelength; therefore a more sensible model should include the small scale dynamics. The Swift-Hohenberg (SH) equation [10] is a phenomenological model equation with the full symmetry of the original problem, and it contains dynamics down to the small scale of the basic wavelength. Various modified forms of the SH equation have been used successfully in studying many different experimental systems, e.g., non-Bousinesq effects, mean flow effects [11], Hopf bifurcation [12,13], and rotating convection [14]. This is the approach we take in this paper.

To mimic the physics of the liquid crystal electroconvection, the modified Swift-Hohenberg equation (MSHE) has to be anisotropic (even at the linear level), and it has to be complex because the initial bifurcation is a Hopf bifurcation. Let $\phi(\vec{x},t)$ be the complex order parameter. We can write the order parameter equation as

$$\partial\phi/\partial t = (\epsilon + i\omega)\phi - \sigma((\partial_x^2 + q_x^2)^2 + b(\partial_x^2 + q_x^2)(\partial_y^2 + q_y^2)$$

$$+ (\partial_y^2 + q_y^2)^2)\phi + iv_g((\partial_x^2 + q_x^2) + a(\partial_y^2 + q_y^2))\phi$$

$$+ g_0|\phi|^2\phi + g_1|\phi|^4\phi. \tag{1}$$

Here, ϵ is the reduced Rayleigh number, ω is the Hopf frequency, $\vec{q} = (q_x, q_y) = |\vec{q}|(\cos\theta, \sin\theta)$, and the length scale of the equation is set by letting $|\vec{q}| = 1$, so the linearly most unstable wavelength $\lambda_0 = 2\pi$. Also b is an anisotropic parameter with the constraint $|b| \leq 2$, and σ is a complex con-
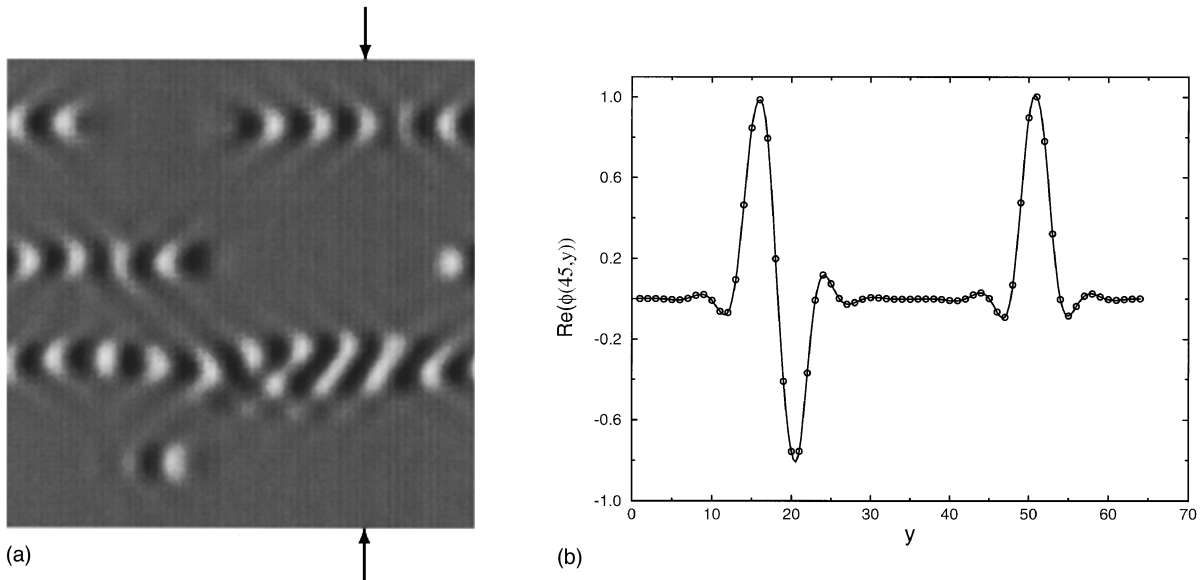
FIG. 1. (a) A 2D snapshot of the field Re[$\phi(x,y)$] for $\epsilon = -0.2$, $a = 1$, $b = 0$, $v_g = 0.5$, $\sigma = 1.5$, $g_0 = 3 + i$, and $g_1 = -2.75 + i$, showing the localized worm structures. (b) A cross section of the 2D pattern shown in (a) at $x = 45$ (indicated by the arrows): Re[$\phi(45,y)$] versus y. The structure on the left side shows the overlapping region of two counterpropagating worms, and the structure on the right side shows the transverse profile of an individual worm.

stant. The first two lines on the right-hand side (RHS) of Eq. (1) represent the linear properties of the electroconvection system, which can be extracted from experiment or linear microscopic theory. It is easy to see that the system is linearly most unstable at $|k_x| = q_x$ and $|k_y| = q_y$ for $\phi \sim \exp(ik_x x + ik_y y)$. The parameter v_g is proportional to the group velocity and a is another anisotropic parameter (when $a = 1$, the group velocity is along the wave-vector direction $\hat{q}$). The last line on the RHS of Eq. (1) contains the nonlinear coupling terms with complex coefficients g_0 and g_1. In general, the nonlinear terms can also be anisotropic; we only include the simplest terms possible here.

Since it is the goal of this paper to find the localized worm state, we focus our attention on the subcritical case [15] where Re(g_0)>0 and Re(g_1)<0. We can easily eliminate the $i\omega$ term in the linear part of the equation by a change of variable $\phi = e^{i\omega t}\phi$, so we will set $\omega = 0$ for now on. There are five real parameters: ϵ, a, b, θ, and v_g and three complex parameters: σ, g_0, and g_1 for this model. We have numerically studied the MSHE extensively in parameter space and identified certain parameter regions where the localized worm state is observed.

To demonstrate the existence of the worm state, we first show the behavior of Eq. (1) for a particular set of parameters: $\epsilon = -0.2$, $a = 1$, $b = 0$, $\theta = 23^o$, $v_g = 0.5$, $\sigma = 1.5$, $g_0 = 3 + i$, and $g_1 = -2.75 + i$. The equation is simulated in systems of size 64×64, 128×64, and 256×64 with periodic boundary conditions using both a second order finite difference method and spectral method with discretization $\Delta x = \Delta y = 0.5, 1.0$ and time step $\Delta t = 0.001, 0.01$. We start the system with random initial conditions with large enough amplitude. The system quickly organizes itself into the worm-like state. A snapshot of the 2D pattern for Re[$\phi(x,y)$] after the initial transient is shown in Fig. 1(a).

In order to show the localization of the worm states in the y direction, a cross section of the 2D pattern [Fig. 1(a)] along the y direction at $x = 45$ is shown in Fig. 1(b). The worm

states travel in the x direction. According to their length, the worm states in our simulation can be divided into two categories, which we call the long worm and the short worm. The length of the short worm does not change with time, and is usually $\sim 3\lambda_0$. Short worms travel in the x direction with constant velocity proportional to v_g. An example of a short worm can be seen near the bottom of Fig. 1(a). The long worm's length grows with time and eventually extends over the whole length of the system because of the periodic boundary condition.

We have tested the sensitivity of the worm pattern to the parameters in our model. We find that there is a finite range of parameters where the worms appear. For example, if we change the value of ϵ while keeping the rest of the parameters unchanged, worms exist for $-0.10 > \epsilon > -0.25$. When ϵ is too small, there is no pattern; and when ϵ is too big, the pattern becomes extended instead. The worm state is quite insensitive to the values of a and b, as long as $a \sim 1$ and $|b| < 2$. For $b = 2$ and $a = 1$, the model becomes isotropic and the worm structure gives way to a time-dependent patchy structure [13]. The velocity v_g is important to give the worm a group velocity. The wave-vector angle θ has to be small enough $\theta \leq 35°$ to make the worm perfectly aligned in the x direction. There are also finite regions in the parameters g_0, g_1, σ where worm states are observed.

The worm states interact strongly with each other. When two short worms collide, they come out of the collision without changing their characteristics. When a short worm collides with a long worm, the short worm sometimes disappears. When two long worms approach each other off center, oblique rolls are excited in the region of their overlap until the worms pass through each other or one of the worms disappears. When two long worms collide head on, they stop each other and form a well defined boundary between them.

For the short worm, because the spatial extent in both directions is about the same order, the formation of the short worm is likely due to strong interaction between the two
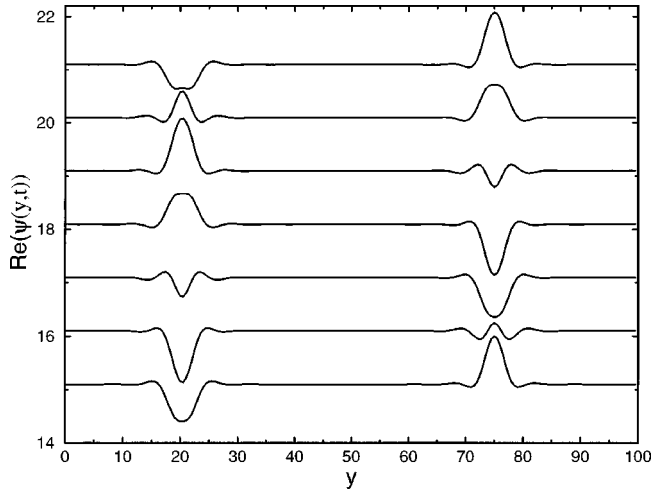
FIG. 2. Space time plot of the field in Eq. (3): Re[$\psi(x,t)$]+$t/4$ versus x for time difference $dt=4$, showing two stationary pulses. The initial condition is random noise with large enough amplitude; the parameters are explained in the text.

directions. However, for the long worms, due to the extendedness of the worm in the x direction, we are able to separate the dependence in the two directions and therefore gain more understanding of the mechanism for the localization in the y direction. Indeed, Fourier analysis of the long worm along the x direction shows that it is a good approximation for assuming the x dependence to be a simple plane wave:

$$\phi(x,y,t)=\psi(y,t)\exp(ik_x x). \tag{2}$$

If we substitute the above ansatz into the original Eq. (1), we obtain a 1D MSHE for $\psi(y,t)$. For simplicity, we set $a=1$ and $b=0$:

$$\partial\psi/\partial t=(\widetilde{\epsilon}+i\widetilde{\omega})\psi-\sigma(\partial_y^2+q_y^2)^2\psi+iv_g(\partial_y^2+q_y^2)\psi$$
$$+g_0|\psi|^2\psi+g_1|\psi|^4\psi, \tag{3}$$

where $\widetilde{\epsilon}=\epsilon-\text{Re}(\sigma)(q_x^2-k_x^2)^2$ and $\widetilde{\omega}=\omega-\text{Im}(\sigma)(q_x^2-k_x^2)^2+v_g(q_x^2-k_x^2)$. $\widetilde{\omega}$ is set to 0 as in 2D.
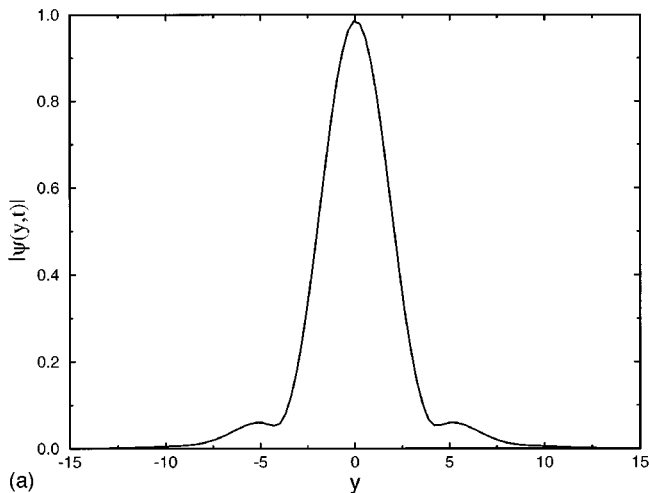
We have studied the above 1D MSHE carefully. The numerical scheme is the same as in the two-dimensional case, and we also start with a random initial condition with sufficient amplitude. In order to compare it to the two-dimensional case, we have set the parameters $\sigma=1.5$, $v_g=0.5$, $g_0=3.0+i$, and $g_1=-2.75+i$ to be the same as in the 2D calculation. We can vary $\widetilde{\epsilon}$ because the value of k_x is undetermined a priori. For $q_y=\sin(\theta)$ with $\theta=23°$, we find a finite range of $\widetilde{\epsilon}$ values, where localized structure is observed $-0.15>\widetilde{\epsilon}>-0.5$. A space-time plot of Re[$\psi(y,t)$] for $\widetilde{\epsilon}=-0.25$ after an initial transient is shown in Fig. 2. It is clear from Fig. 2 that the final state consists of localized pulses. Most remarkably, the pulses are not moving, even in the presence of the group velocity term in Eq. (3).

We find that the pulse solution can be written as

$$\psi(y,t)=A(y)\exp[i\alpha(y,t)], \tag{4}$$

where the amplitude $A(y)$ is independent of time and is localized with a width of $1.5\lambda_0$. With its peak position shifted to $y=0$, the shape of the pulse is symmetric around $y=0$: $A(y)=A(-y)$. The phase of the pulse depends on time linearly:

$$\alpha(y,t)=\alpha_0(y)+\Omega t, \tag{5}$$

with $\Omega=-0.25$. The shape of the time-independent phase $\alpha_0(y)$ is depicted in Fig. 3(b). From Fig. 3(b), we see that the phase is symmetric around $y=0$: $\alpha_0(y)=\alpha_0(-y)$. The phase is nearly constant near the center. Away from the center, the phase is

$$\alpha_0(y)\sim-k_y|y|+\text{const}, \quad |y|>5$$

with $k_y\sim 1$.

As we pointed out earlier in our paper, the existence of a localized state in the subcritical equation with complex coefficient is now well known [2]. However, a stationary localized pulse in the full equation, including the group velocity term, is observed here. If one were able to eliminate the
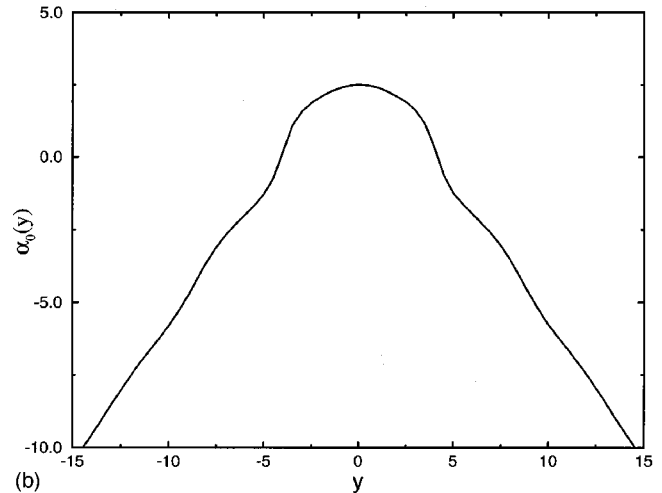
FIG. 3. (a) The amplitude of the 1D pulse shown in Fig. 2: $A(y)$ versus y; (b) the stationary part of the phase of the 1D pulse $\alpha_0(y)$ versus y. See text for explanation.

small scale structure and write the full equation in terms of the amplitude equation, one could use two coupled complex Ginzburg-Landau equations characterizing oppositely moving wave packets. As shown in the work of Brand and Deissler [16], the oppositely moving pulses often pass through each other without altering their own characteristics. Upon tuning the intercoupling between the two oppositely moving pulses, the pulses can form a bound state that does not move in either direction. However, the structure of the bound state is such that the amplitudes of the two oppositely moving pulses are strongly suppressed in their overlap region, which is quite different from our stationary pulse state. Furthermore, in our simulation, no prebound traveling pulse was observed, and the stationary localized state always forms spontaneously as one whole object, which is also consistent with the experiment.

Away form the center, the two halves of the pulse seem to have opposite phase velocity $v_p = \pm \Omega/k_y$. However, k_y is much larger than the linearly most unstable wave number q_y. In addition, the size of the pulse, i.e., the spatial extent of the whole pulse is smaller than $2\pi/q_y$. This clearly shows that the localized pulse observed here is indeed a different structure, which can only be studied using models that include the small scale physics.

In summary, we have constructed a modified Swift-Hohenberg model to explain the formation of the localized worm state observed in electroconvection experiments. For a broad parameter range, we have found a solution of the MSHE that is localized in one direction (y direction) and extended in the other direction (x direction). In the y direction, the amplitude of the worm is maximum at the center and decays rapidly away from the center, The localization of the solution is understood by the discovery of a localized stationary pulse state in 1D, whose existence depends crucially on small scale physics (nonadiabatic effect). In addition, the phase inside the worm, as shown in Fig. 3(b), cannot be described by the linearly most unstable modes $\vec{q}_{\pm} = (q_x, \pm q_y)$. In the x direction, the long worm expands while moving with the group velocity.

Our results may be tested experimentally and also provide a link between experiment and quantities accessible to the microscopic theory. In particular, we find that the worm state occurs for subcritical parameters. This means that the onset of the (presumably unstable) extended plane wave state is subcritical, with discontinuities in the amplitude, etc. This simple state, although unstable, should be accessible to calculations based on the microscopic theory. Our model shows that the maximum amplitude of the localized structures in the worm state (a quantity much more difficult to calculate from the full equations) also jumps discontinuously at the onset: this can be tested explicitly by experiment, and in this sense the experimental transition is predicted to be subcritical [17]. We also find that the phase structure inside the worm is quite different from that described by the linearly unstable wave vectors: this can also be checked by detailed experimental study of the worm structure.

In addition, our theory can be used to explain the transition between the spatially extended STC state at small conductivity and the worm state at higher conductivity. The transition can be simply related to the supercritical to subcritical transition in our model where $\text{Re}(g_0)$ changes sign. The study of this transition and the exploration of the parameter space will be published elsewhere.

The discovery of the worm state in the MSHE proposed in this paper is an important step towards fully understanding the worm states, including questions such as the nucleation and interaction of the worms. Evidently, further experimental and theoretical work is needed to fully comprehend these fascinating phenomena in electroconvection.

---

[1] E. Moses, F. Fineberg, and V. Steinberg, Phys. Rev. A **35**, 2757 (1987); R. Heinrichs, G. Ahlers, and D. S. Cannell, *ibid.* **35**, 2761 (1987).

[2] O. Thual and S. Fauve, J. Phys. (France) **49**, 1829 (1988).

[3] H. Riecke, Phys. Rev. Lett. **68**, 301 (1992).

[4] R. J. Deissler and H. R. Brand, Phys. Lett. A **146**, 252 (1990).

[5] P. Kolodner, D. Bensimon, and C. Surko, Phys. Rev. Lett. **60**, 1723 (1988); J. Niemela, G. Ahlers, and D. Cannell, *ibid.* **64**, 1365 (1990); P. Kolodner, Phys. Rev. E **50**, 2731 (1994).

[6] V. Steinberg, E. Moses, and J. Fineberg, Nucl. Phys. B **2**, 109 (1987).

[7] E. Bodenschatz, D. S. Cannell, R. Ecke, Y. C. Hu, K. Lerman, and G. Ahlers, Physica D **61**, 77 (1992).

[8] M. Dennin, G. Ahlers, and D. S. Cannell, Phys. Rev. Lett. **77**, 2475 (1996); Science **272**, 388 (1996).

[9] M. Dennin, M. Treiber, L. Kramer, G. Ahlers, and D. S. Cannell, Phys. Rev. Lett. **76**, 319 (1996); M. Treiber and L. Kramer, Mol. Cryst. Liq. Cryst. **261**, 311 (1995).

[10] J. B. Swift and P. C. Hohenberg, Phys. Rev. A **15**, 319 (1977).

[11] H. S. Greenside and M. C. Cross, Phys. Rev. A **31**, 2492 (1985).

[12] T. Ohta and K. Kawasaki, Physica D **27**, 21 (1987).

[13] M. Bestehorn, R. Friedrich, and H. Haken, Z. Phys. B **75**, 262 (1989); **77**, 151 (1989); M. Bestehorn and H. Haken, Phys. Rev. A **42**, 7195 (1990).

[14] M. C. Cross, Y. Tu, and D. Meiron, CHAOS **4**, 607 (1994).

[15] A study for the supercritical case $\text{Re}(g_0) < 0$ has found no worm structure.

[16] H. R. Brand and R. J. Deissler, Phys. Rev. Lett. **63**, 2801 (1989); Phys. Rev. A **44**, R3411 (1991).

[17] By contrast, global measured averages, such as the Nusselt number, may be continuous at onset if the separation of the worms diverges here. In this case the transition to chaos may also show properties characteristic of a continuous, supercritical bifurcation such as scaling behavior.